REPORT DOCUMENTATION PAGE

Form Approved
OMB No. 0704-0188

1. REPORT DATE *(DD-MM-YYYY)*	**2. REPORT TYPE**	**3. DATES COVERED** *(From - To)*
26-01-2009	Journal Article	

4. TITLE AND SUBTITLE

Methodology and Historical Perspective of a Hall Thruster Efficiency Analysis

5a. CONTRACT NUMBER

5b. GRANT NUMBER

5c. PROGRAM ELEMENT NUMBER

6. AUTHOR(S)
Daniel L. Brown (ERC); C. William Larson, Brian E. Beal (AFRL/RZSS); Alec D. Gallimore (University of Michigan)

5d. PROJECT NUMBER

5e. TASK NUMBER

5f. WORK UNIT NUMBER
33SP0708

7. PERFORMING ORGANIZATION NAME(S) AND ADDRESS(ES)

Air Force Research Laboratory (AFMC)
AFRL/RZSS
1 Ara Road
Edwards AFB CA 93524-7013

8. PERFORMING ORGANIZATION REPORT NUMBER

AFRL-RZ-ED-JA-2009-023

9. SPONSORING / MONITORING AGENCY NAME(S) AND ADDRESS(ES)

Air Force Research Laboratory (AFMC)
AFRL/RZS
5 Pollux Drive
Edwards AFB CA 93524-7048

10. SPONSOR/MONITOR'S ACRONYM(S)

11. SPONSOR/MONITOR'S NUMBER(S)
AFRL-RZ-ED-JA-2009-023

12. DISTRIBUTION / AVAILABILITY STATEMENT

Approved for public release; distribution unlimited (PA #09075).

13. SUPPLEMENTARY NOTES
For publication in the AIAA Journal of Propulsion and Power.

14. ABSTRACT

A Hall thruster performance architecture was developed based on separation of the total thrust directed along thruster centerline into mass-weighted and momentum-weighted terms. With this formulation, the anode thrust efficiency equation was analytically decomposed to explicitly account for the effects of energy conversion losses, plume divergence, and the velocity distribution function of the propellant jet. Thruster efficiency is defined as the product of (1) energy efficiency, (2) propellant efficiency, and (3) beam efficiency. Energy efficiency comprises losses due to ionization processes and losses that manifest as Joule heating of the thruster, and contains no information about the vector properties of the jet. Propellant efficiency incorporates losses from dispersion in the jet composition, and is unity for 100% ionization to a single ion species. The effect of neutrals on dispersion of the jet VDF in propellant efficiency is introduced in the neutral-gain utilization. The beam efficiency accounts for divergence of the jet, and is ideal when the ion velocity vectors are parallel to the thrust axis. Plume divergence is defined as a momentum-weighted term, and the approximation as a charge-weighted term is characterized. The efficiency architecture is derived from first principles and is applicable to all propulsion employing electrostatic acceleration, including Hall thrusters and ion engines. Similarities and distinctions to several past methodologies are discussed, including past ion engine analyses, early Russian performance studies, and contemporary architectures. Thrust and far-field plume measurements of a 6 kW laboratory Hall thruster are used to study the analysis capability in characterizing performance loss mechanisms.

15. SUBJECT TERMS

16. SECURITY CLASSIFICATION OF:			**17. LIMITATION OF ABSTRACT**	**18. NUMBER OF PAGES**	**19a. NAME OF RESPONSIBLE PERSON**
					Dr. Brian E. Beal
a. REPORT	**b. ABSTRACT**	**c. THIS PAGE**	SAR	31	**19b. TELEPHONE NUMBER** *(include area code)*
Unclassified	**Unclassified**	**Unclassified**			N/A

Methodology and Historical Perspective of a Hall Thruster Efficiency Analysis

Daniel L. Brown[1], C. William Larson[2], Brian E. Beal[3]
Air Force Research Laboratory, Edwards AFB, CA 93524-7680

and

Alec D. Gallimore[4]
Plasmadynamics and Electric Propulsion Laboratory
University of Michigan, Ann Arbor, MI, 48109, USA

A Hall thruster performance architecture was developed based on separation of the total thrust directed along thruster centerline into mass-weighted and momentum-weighted terms. With this formulation, the anode thrust efficiency equation was analytically decomposed to explicitly account for the effects of energy conversion losses, plume divergence, and the velocity distribution function of the propellant jet. Thruster efficiency is defined as the product of (1) energy efficiency, (2) propellant efficiency, and (3) beam efficiency. Energy efficiency comprises losses due to ionization processes and losses that manifest as Joule heating of the thruster, and contains no information about the vector properties of the jet. Propellant efficiency incorporates losses from dispersion in the jet composition, and is unity for 100% ionization to a single ion species. The effect of neutrals on dispersion of the jet VDF in propellant efficiency is introduced in the neutral-gain utilization. The beam efficiency accounts for divergence of the jet, and is ideal when the ion velocity vectors are parallel to the thrust axis. Plume divergence is defined as a momentum-weighted term, and the approximation as a charge-weighted term is characterized. The efficiency architecture is derived from first principles and is applicable to all propulsion employing electrostatic acceleration, including Hall thrusters and ion engines. Similarities and distinctions to several past methodologies are discussed, including past ion engine analyses, early Russian performance studies, and contemporary architectures. Thrust and far-field plume measurements of a 6 kW laboratory Hall thruster are used to study the analysis capability in characterizing performance loss mechanisms.

---

[1] Research Scientist, ERC Inc.; Ph.D. Candidate, University of Michigan, Plasmadynamics and Electric Propulsion Laboratory; Daniel.Brown@edwards.af.mil. AIAA Student Member.

[2] Research Scientist, Spacecraft Propulsion Branch, AFRL/RZSS; Carl.Larson@edwards.af.mil. AIAA Senior Member.

[2] Group Lead – High Power Electric Propulsion Group, Spacecraft Propulsion Branch, AFRL/RZSS; Brian.Beal@edwards.af.mil. AIAA Member.

[4] Laboratory Director, Plasmadynamics and Electric Propulsion Laboratory; Professor, Department of Aerospace Engineering; Associate Dean, Horace H. Rackham School of Graduate Studies, Alec.Gallimore@umich.edu. Associate Fellow AIAA.

Nomenclature

A = spherical shell surface area element in the plume
E_1 = voltage exchange parameter
E_2 = mass exchange parameter
$\mathbf{F}$ = thrust density vector in the plume
f^*_j = normalized ion mass flow fraction of jth ion species
$\mathscr{F}$ = Faraday constant, 96,485 coulombs/mol of charge
$f(\mathbf{v})$ = velocity distribution function of ions and neutrals
g = Earth's gravitational constant at sea level, 9.806 m/s^2
I_d = anode discharge current
I_{Beam} = integrated beam current
I_{Axial} = axial component of beam current parallel to thruster centerline
I_{sp} = specific impulse
j = propellant charge state index, 0, 1, 2, 3, etc. for Xe^0,Xe^{+1},Xe^{+2},Xe^{+3}
$J(\theta)$ = current density in the plume at angular position θ
$\dot{m}$ = anode propellant mass flow rate, where $\sum \dot{m}_j = \dot{m}$ for j=0 to the jth ion species
$\dot{m}(\theta)$ = anode propellant mass flow rate at angular position θ
$\dot{m}_i$ = mass flow rate of ions, where $\sum \dot{m}_j = \dot{m}_i$ for j=1 to the jth ion species
$\dot{m}_j$ = mass flow rate of jth propellant species
$\mathscr{M}$ = molecular weight of propellant (Xe = 0.1313 kg/mol)
P_d = discharge power to anode = $V_d I_d$
P_{jet} = jet power
P_{min} = minimum power loss to sustain ionization
Q = average charge of propellant ions
q = unit of charge, 1.609 x 10^{-19} Coulombs
r = fraction of electron current to the anode, electron recycle fraction
(1-r) = current utilization, fraction of ion beam current = I_{Beam} / I_d
r_{min} = minimum fraction of electron current required to sustain discharge
T = component of thrust vector directed along thruster centerline
V_a = most probable ion acceleration voltage
V_d = anode discharge voltage
v_j = exit speed of jth species
$\overline{\mathbf{v}}$ = average exit velocity of the VDF over velocity space d$\mathbf{v}$ at angular position θ
$\overline{v}(\theta)$ = radial component of $\overline{\mathbf{v}}$ in hemispherical coordinates from thruster centerline at angular position θ
$\overline{v}$, $\overline{v^2}$ = average propellant velocity, squared propellant velocity
$\overline{v_i}$, $\overline{v_i^2}$ = average ion velocity, squared ion velocity
y_j = normalized speed ratio of the jth species = $v_j / |v_1|$
Zj = ion charge state = 1, 2, 3 for Xe^{+1}, Xe^{+2}, Xe^{+3}
β = fractional loss of acceleration potential
$(1-\beta)$ = voltage utilization, V_a / V_d
δV_j = acceleration potential of jth ion species
ε_j = ionization potential of jth ion species (12, 33, 65 eV from neutral ground state for Xe)

η_E = energy efficiency = (1-β) (1-r)
η_A = anode thrust efficiency
θ = angular position in the plume, θ=90° on thrust axis
λ = plume momentum divergence half-angle, λ=0° on thrust axis
ρ = radial coordinate in the spherical coordinate system
Φ_m = mass utilization, ion mass flow fraction at exit, $\sum \dot{m}_j / \dot{m}$ for j=1 to the jth ion species
$\Phi_{n\text{-}g}$ = neutral gain utilization resulting from the bulk and thermal speed of neutral propellant
Φ_P = propellant efficiency, losses due to dispersion of the VDF = $\Phi_m \Phi_{N\text{-}G} \Phi_q$
Φ_q = charge utilization
χ = output moles of ion charge per input moles of propellant = $\Phi_m Q = I_{Beam} \mathcal{M} / (\dot{m} \mathcal{F})$
Ψ_B = beam efficiency, divergence loss component of thrust
Ω_j = normalized ion species current fraction = $f^*_j Z_j / Q$
ζ_j = normalized ion species number density fraction ~ $f^*_j Z_j^{-1/2}$

$< >_m$ = mass weighted average quantity in the plume ($0<\theta<\pi$)
$< >_{mv}$ = momentum weighted average quantity in the plume ($0<\theta<\pi$)
$< >_J$ = charge flux weighted average quantity in the plume ($0<\theta<\pi$)

I. Introduction

Standardization of experimental methods, facilities, diagnostic apparatus, and efficiency analysis has previously been proposed in the electric propulsion community.[1] An efficiency architecture is presented that is based on a consistent set of definitions, conservation of energy, conservation of mass and charge, and Newton's Second Law. The relationships between Hall thruster performance data, telemetry (V_a, I_a, and $\dot{m}$), and plume measurements are summarized and new correlations are developed.

In this paper, we present the basis for analytical separation of anode thrust efficiency into the product of energy efficiency, propellant efficiency, and beam efficiency, which are less than unity under all operating conditions. Separating utilization efficiencies in this manner isolates performance losses in terms of energy losses that lead to Joule heating, dispersion of the jet velocity distribution function (VDF), and loss of thrust due to plume divergence. While these processes are physically coupled, the effects on performance may be mathematically isolated.

Historical perspective of early ion engine analyses, methodologies developed in the former Soviet Union, and a brief description of contemporary efficiency models are discussed in relation to the presented architecture. The architecture is distinctive in formulating the axial component of thrust as the product of mass-weighted and

momentum-weighted quantities, and introduces a new definition of propellant utilization that incorporates multiple ion species and the effects of neutral propellant. Thruster performance parameters, including thrust to power (T/P) and specific impulse (Isp), are formulated in terms of utilization efficiencies to provide a higher level of confidence in comparisons between plume measurements and thrust measurements. Experimental thrust and plume measurements from a 6 kW laboratory model Hall thruster are studied to illustrate the fidelity of the proposed analytical model and to demonstrate the utility of combining results from a set of diagnostics in determining Hall thruster performance. Power losses are studied using energy efficiency and compared to the minimum power required to sustain the discharge ion species composition.

II. Historical Perspective and Recent Efforts

Investigations of ion acceleration and electron transport using Hall thruster technology began in the early 1960s in the United States and former Soviet Union.[2,3,4,5,6,7,8,9,10,11,12] The focus of US electric propulsion research shifted primarily to ion engine technology in the early 1970s[13], whereas investigations in the USSR continued Hall thruster advancements throughout the following decades.[14,15,16]

Analytical factorization of ion engine thruster efficiency was described as early as 1975 by Masek *et al.* in a review of ion engine performance.[17] Thrust efficiency was factored into the product of energy efficiency and propellant utilization efficiency using Newton's Second Law, with terms accounting for losses due to doubly charged ions and beam divergence. However, the derivation was condensed and an explanation for the treatment of beam divergence and multiply charged ions was not presented. The methodology was not widely adopted or cited in the ion engine community and is absent in modern analysis.

In the 1990s, the manifestation of Russian Hall thruster technology in the Western and Japanese spacecraft communities catalyzed a resurgence of Hall thruster research.[18,19,20,21,22,23] Technology transfer that began in the early 1990s brought invaluable benefits and advancements to Western Hall thruster development, but much of the earlier Soviet progress in Hall thruster research that was published in the Russian language was not translated. The limited availability of translated documents from this extensive literature inevitably impeded the transmission of knowledge and progress. As a result, several important contributions from Russian research have not been widely disseminated in the West, including the analytical factorization of anode thrust efficiency.

Factorization of Hall thruster efficiency was outlined in a manual on stationary plasma engines by Belan, Kim, Oranskiy, and Tikhononv from the Kharkov Aviation Institute in 1989.[24] This seminal document was later referenced and the performance methodology summarized by Bugrova *et al.* without explicitly stating the nature of the earlier derivation.[25] Kim's highly cited 1998 paper on processes that determine Hall thruster efficiency[26] and other contemporary publications[27,28,29] continued the elaboration of the Kharkov Aviation Institute methodology. These approaches showed similarities to the analysis presented here, and demonstrated relationships between experimental variables and plasma phenomena that affect thruster performance.

A textbook by Grishin and Leskov analyzed thruster performance based on energy efficiency and thrust efficiency.[30] The ratio of thrust efficiency to energy efficiency was asserted to describe the velocity dispersion in magnitude and direction. This ratio will be derived from first principles in the following section, where it will become apparent that the ratio is equivalent to beam efficiency and propellant efficiency, which capture losses resulting from plume divergence, incomplete ionization, and the production of multiply charged ions.

The term *propellant utilization efficiency* has been used in at least three different ways in the literature. Most commonly as (1) the ionization fraction, as (2) the fraction of momentum carried by ions[14], or as (3) the ratio of output moles of charge to the input moles of propellant[31], which is equivalent to the product of the ionization fraction and average ion charge. While the definitions of voltage and current utilization are standardized, a consistent description of propellant utilization has not emerged.

In the post-1990 era, numerous efficiency analysis frameworks and modifications have been proposed, [32,33,34,35,36,37,38,39,40] including notable studies by Komurasaki[41], Ahedo[42], and Hofer[43,44]. The difference between the proposed architecture with past ion engine studies, the analytical factorization in Russian literature, and the post-1990 methodologies varies in each case. Dissimilarities arise due to varying levels of completeness regarding the treatment of multiply charged ions, beam divergence, and the effect of neutral propellant on dispersion of the jet VDF. In some instances, the effects of these loss mechanisms are neglected or inserted as a utilization efficiency without rigorously factoring the term from the anode thrust efficiency equation. Utilization efficiencies in the performance model presented in this paper are analytically separated from the thrust efficiency and are formulated to minimize the introduction of new terminology. The primary differences with all previous methodologies is quantifying the effect of neutrals on dispersion of the VDF in the neutral-gain utilization and decomposing total

thrust into the product of mass-weighted and momentum-weighted quantities. Three appendices are included to define plume averaged terms and detail the derivation of propellant efficiency and beam efficiency.

This analytical tool is not meant to predict Hall thruster physics or plasma properties in the same manner as a computational model. Numerical simulations typically determine plasma properties throughout the plume and/or performance attributes based on a particle source mode. In contrast, the analytical model employs performance measurements and bulk plume characteristics to experimentally determine physical processes and relationships that are difficult to measure directly.

III. Hall Thruster Performance Architecture

A. Decoupling Energy Efficiency, Beam Efficiency, and Propellant Efficiency

The total thrust generated by a Hall thruster is a primarily a function of electromagnetic forces, and to a much lesser degree gasdynamic forces. Downstream of the primary ionization and acceleration regions, the total resultant thrust may be found from Eq. (1) through integration of the thrust density vector throughout the plume.

$$T\,\hat{\rho} = \iint \mathbf{F}\cdot\hat{\rho}\;\mathrm{d}A \tag{1}$$

This idealized description suffers from numerous experimental difficulties and uncertainties. Although Eq. (1) may be valid in the space environment, facility effects inherent in ground tests result in significant scattering in the plume and potentially increased thrust from neutral ingestion. Measurements of thrust density throughout the HET plume are extremely difficult, but may be viable using an impact target plate.[45]

The conventional inverted pendulum thrust stand measures the component of thrust directed along the thruster centerline axis. Careful thruster alignment and uniform propellant injection generally result in an axisymmetric plume with negligible deviations between the resultant thrust vector direction and the thruster centerline axis. For an axisymmetric plume, the steady-state scalar component of thrust directed along thruster centerline is formulated in Eq. (2). The total thrust may be factored into the product of mass flow, mass-weighted average velocity, and momentum-weighted average divergence using the definitions listed in Appendix A. Thrust is often defined as $\dot{m} < \overline{v_i} > <\cos(\lambda)>$ without mathematically separating terms from the thrust integral.

$$T = 2\pi R^2 \int_0^{\pi/2} \dot{m}(\theta)\;\overline{v}(\theta)\cos(\theta)\sin(\theta)\,\mathrm{d}\theta \;= \dot{m} < \overline{v} >_m < \cos(\theta) >_{mv} \tag{2}$$

In Eq. (3), the standard definition of anode thrust efficiency is expressed in terms of thruster telemetry and measured thrust. Anode efficiency is decomposed into the product of energy efficiency, propellant efficiency, and beam efficiency using the definition of jet kinetic energy, Newton's Second Law, and the mass-weighted average squared velocity as defined in Eq. (A-5) of Appendix A.

$$\eta_A = \frac{\frac{1}{2}T^2}{\dot{m}P_d} = \frac{\frac{1}{2}\left(\dot{m} < \overline{v} >_m < \cos(\theta) >_{mv}\right)^2}{\dot{m}P_d} = \eta_E \, \Phi_P \, \Psi_B \tag{3}$$

Energy efficiency in Eq. (4) characterizes the conversion of input anode electrical energy to jet kinetic energy, and contains all information about losses that ultimately appear as Joule heating of the channel walls and thruster body, radiation from the jet, and frozen ionization losses in the plume. In this analysis, the jet power accounts for the energy of neutral propellant, whereas most definitions include only beam ion energy.

$$\eta_E = \frac{P_{jet}}{P_d} = \frac{\frac{1}{2}\dot{m} < \overline{v^2} >_m}{V_d I_d} \tag{4}$$

Jet momentum losses due to beam divergence are quantified using the momentum-weighted average cos(θ) in Eq. (5). This formulation is similar to the focusing efficiency described by Kim, but is naturally expressed as a momentum-weighted average quantity from the formulation of thrust.

$$\Psi_B = < \cos(\theta) >_{mv}^2 \tag{5}$$

Propellant efficiency in Eq. (6) is the mathematical relationship between the particle momentum and the jet kinetic energy. It contains all loss information associated with dispersion of the jet VDF due to incomplete ionization and the presence of multiple ion species with widely varying velocities. This ratio is unity for 100% ionization to a single ion species.

$$\Phi_P = \frac{< \overline{v} >_m^2}{< \overline{v^2} >_m} \tag{6}$$

The factors affecting propellant efficiency, energy efficiency, and beam efficiency will be discussed in the following sections. Propellant efficiency will be decomposed into mass and charge utilization efficiencies, and the neutral-gain utilization is introduced to characterize the effect of neutral propellant on dispersion of the VDF. Next, energy efficiency is separated into the product of voltage utilization and current utilization using χ. Beam efficiency

will then be analyzed in terms of the distinction between momentum-weighted divergence and current-weighted plume divergence.

B. Decoupling Mass, Charge, and Neutral-Gain Utilization from Propellant Efficiency

The influence of non-uniform velocity distribution on propellant efficiency due to multiple ion species and unionized propellant is expressed in Eq. (7). Propellant efficiency is separated into the product of mass utilization, charge utilization, and neutral-gain utilization using the definitions in Appendix B. The propellant efficiency is separated in this way to maintain a consistent definition of mass utilization and charge utilization with previous methodologies[43], and isolate effects resulting from the bulk and thermal speed of neutrals.

$$\Phi_P = \left(\frac{<\bar{v}_i>_m^2}{<\overline{v_i^2}>_m} \right) \left(\frac{<\bar{v}>_m^2}{<\bar{v}_i>_m^2} \frac{<\overline{v_i^2}>_m}{<\overline{v^2}>_m} \right) = \Phi_q \Phi_m \Phi_{N\text{-}G} \tag{7}$$

The standard definition of charge utilization is formulated from the first term in brackets in Eq. (7). Charge utilization is expressed in Eq. (8) using species current fractions as obtained from an ExB probe and is unity for ionization to a single ion species. Charge utilization is also written using ion species mass flow fractions in Eq. (8). Ion mass flow fractions are defined according to Eq. (9).

$$\Phi_q = \left(\frac{<\bar{v}_i>_m^2}{<\overline{v_i^2}>_m} \right) = \frac{\left(\sum_{j=1} \frac{\Omega_j}{\sqrt{Z_j}} \right)^2}{\sum_{j=1} \frac{\Omega_j}{Z_j}} = \frac{\left(\sum_{j=1} f_j^* \sqrt{Z_j} \right)^2}{\sum_{j=1} f_j^* Z_j} \tag{8}$$

$$f_j^* = \frac{\dot{m}_j}{\sum_{j=1} \dot{m}_j} \tag{9}$$

It is important to note the distinction between ion current fractions, ion flow fractions, and ion species fractions. Ion current fraction is determined directly from ExB probe traces. Ion species fractions are based on particle number density, and are commonly reported for incorporation in numerical simulations. The ion flow fraction is a more suitable figure of merit for experimental plume studies, since it is related to the ion species momentum in the plume. The average ion charge Q in Eq. (10) is expressed in terms of ion current fractions, ion flow fractions, and ion species fractions.

$$Q = \sum_{j=1} f_j^* \, Z_j = \left(\sum_{j=1} \frac{\Omega_j}{Z_j} \right)^{-1} = \frac{\sum_{j=1} \zeta_j \, Z_j^{3/2}}{\sum_{j=1} \zeta_j \, Z_j^{1/2}} \tag{10}$$

The mass utilization and neutral-gain utilization are developed from the second term in brackets in Eq. (7). Mass utilization is defined as the ratio of ion mass flow rate to anode mass flow rate in Eq. (11), and is calculated using beam current from a Faraday probe in conjunction with the average ion charge from an ExB probe.

$$\Phi_m = \frac{\sum_{j=1} \dot{m}_j}{\sum_{j=0} \dot{m}_j} = \frac{\dot{m}_i}{\dot{m}} = \frac{I_{Beam}}{\dot{m} \, Q} \frac{\mathscr{M}}{\mathscr{F}} \tag{11}$$

The effects of neutral propellant on dispersion of the jet VDF are quantified in Eq. (12). This term is always greater than one, and is indicative of the thrust and energy gained due to the speed of the neutrals. The neutral-gain utilization is a strong function of the normalized neutral speed and mass utilization. The normalized neutral speed is typically less than 0.05 for most Hall thrusters and operating conditions, which results in a neutral-grain utilization of less than 1.02. Neutral-gain utilization is expected to increase for low voltage, high power thruster operation and anode propellant injection with a large bulk axial velocity component. Minimizing this utilization is critical for high performance operation, since it increases with decreased ionization and decreased neutral residence time in the discharge channel.

$$\Phi_{N\text{-}G} \approx 1 + 2 \, y_0 \, \frac{(1 - \Phi_m)}{\Phi_m \sqrt{Q \, \Phi_q}} \tag{12}$$

The factorization of propellant efficiency is detailed in Appendix B, along with a more detailed characterization of the neutral-gain utilization for variation in y_0, Φ_m, and ion species composition.

C. Decoupling Voltage and Current Utilization from Energy Efficiency

Energy efficiency is factored in Eq. (13) as the product of voltage utilization and current utilization. It is convenient to introduce χ, which is defined in Eq. (14) as the ratio of output moles of charge to input moles of propellant. Although χ cancels in the energy efficiency term, it is shown in Equations (17) and (18) to reveal the physical nature of the voltage and current utilization inherent in the thrust efficiency.

$$\eta_E = \frac{\frac{1}{2}\dot{m} < \overline{v^2} >_m}{P_d} = \left[\frac{\frac{1}{2} < \overline{v^2} >_m}{\frac{\mathcal{F}}{\mathcal{M}} V_d}\right]\left[\frac{\dot{m}}{I_d}\frac{\mathcal{F}}{\mathcal{M}}\right] = \left[\chi(1-\beta)\right]\left[\frac{(1-r)}{\chi}\right] = (1-\beta)(1-r) \tag{13}$$

where, by definition

$$\chi = \frac{\sum_{j=1} \dot{m}_j Z_j}{\sum_{j=0} \dot{m}_j} = \frac{\sum_{j=1} \dot{m}_j \sum_{j=1} f_j^* Z_j}{\dot{m}} = \Phi_m \; Q \tag{14}$$

Equation (15) transforms the first term in brackets of Eq. (13) into an expression that contains explicit utilization of acceleration potential for each ion species, $\delta V_j/V_d$. An ExB probe measurement of ion mass flow fractions and estimation of ion acceleration potentials would enable a voltage utilization to be calculated for each ion species. The ratio of average particle specific kinetic energy to average ion specific kinetic energy in Eq. (15) is shown to be approximately equal to Φ_m in Eq. (16). The bracketed quantity in Eq. (16) is very close to unity under all reasonable conditions of Hall thruster operation due to the low value of y_0 in the numerator, since $y_0^2 (1-\Phi_m) < 1x10^{-4}$ for experimental measurements of $y_o < 0.05$.[46,47] Thus, the approximation, $<v^2>_m/<v_i^2>_m \approx \Phi_m$ is accurate to better than one in ten thousand.

$$\frac{\frac{1}{2} < \overline{v_i^2} >_m}{\frac{\mathcal{F}}{\mathcal{M}} V_d} \frac{< \overline{v^2} >_m}{< \overline{v_i^2} >_m} \approx \frac{\frac{1}{2}\Phi_m}{\frac{\mathcal{F}}{\mathcal{M}} V_d} \quad \sum_{j=1}\left(\frac{\dot{m}_j}{\dot{m}_i} v_j^2\right) = \Phi_m \quad \sum_{j=1}\left(f_j^* Z_j \frac{\delta V_j}{V_d}\right) \tag{15}$$

where,

$$\frac{< \overline{v^2} >_m}{< \overline{v_i^2} >_m} = \frac{\sum_{j=0}\left(\frac{\dot{m}_j}{\dot{m}} v_j^2\right)}{\sum_{j=1}\left(\frac{\dot{m}_j}{\dot{m}_i} v_j^2\right)} = \Phi_m \left[1 + \frac{y_0^2 \left(1-\Phi_m\right)}{\chi}\right] \approx \Phi_m \tag{16}$$

$$v_j = \sqrt{2 Z_j \, \delta V_j \left(\frac{\mathcal{F}}{\mathcal{M}}\right)} \tag{17}$$

To simplify the analysis, all ions are considered to be created in the same zone whose length is small compared to the acceleration length, such that $V_a = \delta V_j \approx$ constant. Previous investigations by Kim[48] and King[49] found that species dependent energy to charge ratios varied by tens of volts using different types of energy analyzers. This

variation in energy to charge ratio is less than 10% of the typical discharge voltage. According to Hofer[50], the approximation will have a negligible effect on accuracy since the plume is predominantly composed of singly ionized xenon. The velocity of neutrals and each ion species is approximated with a delta function distribution of velocities, such that the ion species kinetic energies are proportional to their charge and the ion velocity ratio magnitudes are $|y_j|=(Z_j)^{1/2}$. To the author's knowledge, this approximation is consistent with all other performance architectures. Therefore, the most probable ion acceleration potential, V_a, as measured with a retarding potential analyzer (RPA) enables the first term in brackets of Eq. (13) to be expressed in terms of the average voltage utilization efficiency and χ in Eq. (18). The average voltage utilization in Eq. (18) compares the most probable potential gained by ions with the applied anode potential, and is unity for ionization at the anode face where ions are accelerated through the entire anode potential.

$$\frac{\frac{1}{2}<\overline{v^2}>_m}{\frac{\mathcal{F}}{\mathcal{M}}V_d} \approx \Phi_m \frac{V_a}{V_d}\sum_{j=1}\left(f_j^* Z_j\right) = \Phi_m (1-\beta) Q = (1-\beta)\chi \tag{18}$$

The second bracketed term in Eq. (13) is transformed in Eq. (19) into an expression containing the current utilization efficiency and χ. Current utilization efficiency is the fraction of cathode electron flow that electrically neutralizes the accelerated positive ions in the plume, and is calculated as the ratio of ion beam current to discharge current.

$$\frac{\dot{m}}{I_d}\frac{\mathcal{F}}{\mathcal{M}} = \frac{\dot{m}(\mathcal{F}/\mathcal{M})\chi}{I_d}\frac{1}{\chi} = \frac{I_{Beam}}{I_d}\frac{1}{\chi} = \frac{(1-r)}{\chi} \tag{19}$$

$$I_{Beam} = \sum_{j=1}\dot{m}_j Z_j \frac{\mathcal{F}}{\mathcal{M}} = \dot{m}\chi\frac{\mathcal{F}}{\mathcal{M}} \tag{20}$$

Electrons recycled to the anode ionize neutral propellant and sustain dissipative plasma processes. The minimum power required to produce a given ion species composition is expressed in Eq. (21). Based on the minimum power requirement, the minimum recycled electron current in a Hall thruster discharge may be determined as a function of the applied voltage between the anode and cathode. The minimum recycled electron current fraction in Eq. (22) shows that increased discharge voltage, and hence increased recycled electron energy, reduces the minimum recycled electron current. Theoretically, a stream of single electrons may deposit the minimum power to produce a cascade of ionization. Power from recycled electrons in excess of P_{min} is lost by Joule heating processes

to the plasma and channel walls. When combined with the total power loss estimates from energy efficiency, this places an upper limit on Joule heating losses to the walls amounting to $(1-\eta_E-r_{min})P_d$.

$$P_{min} = \sum_{j=1} \left(\dot{m}_j \, \varepsilon_j \right) = \dot{m} \Phi_m \sum_{j=1} \left(f_j^* \, \varepsilon_j \right) \tag{21}$$

$$r_{min} = \frac{P_{min} \, / V_d}{I_d} = \frac{\dot{m} \Phi_m}{P_d} \sum_{j=1} \left(f_j^* \, \varepsilon_j \right) \tag{22}$$

D. Evaluating Plume Divergence Losses in Beam Efficiency

The momentum-weighted average plume divergence is defined in Eq. (23) as the ratio of the measured thrust component directed along the thruster centerline to the theoretical thrust achieved when all ions are traveling parallel to thruster centerline. Momentum losses associated with plume divergence may be calculated with knowledge of the input mass flow, measured thrust, and the mass-weighted average velocity.

$$\Psi_B = <\cos(\theta)>_{mv}^2 = \left(\frac{T}{\dot{m} <\bar{v}>_m} \right)^2 \tag{23}$$

The value $<\cos(\theta)>^2$ has been used in previous analyses to describe plume focusing[26], but there has not been a consistent method to calculate the effect of plume momentum divergence on thrust. This is primarily due to the difficulty of measuring particle velocity throughout the plume. Charge divergence in the plume is indicative of off-axis velocity losses in thrust, and is a useful alternative for experimental characterization of performance losses due to plume divergence. The momentum-weighted average divergence is approximated as the charge-weighted average divergence in Eq. (24) for an axisymmetric plume, which enables calculation of off-axis cosine losses in Eq. (25) using the ratio of the axial component of beam current to total beam current as measured by a Faraday probe.

$$<\cos(\theta)>_{mv}^2 = \left(\frac{2\pi R^2 \int_0^{\pi/2} \left(\frac{\dot{m}(\theta)\bar{v}(\theta)}{J(\theta)} \right) J(\theta)\cos(\theta)\sin(\theta)\,d\theta}{2\pi R^2 \int_0^{\pi/2} \left(\frac{\dot{m}(\theta)\bar{v}(\theta)}{J(\theta)} \right) J(\theta)\sin(\theta)\,d\theta} \right)^2 \cong \left(\frac{2\pi R^2 \int_0^{\pi/2} J(\theta)\cos(\theta)\sin(\theta)\,d\theta}{2\pi R^2 \int_0^{\pi/2} J(\theta)\,\sin(\theta)\,d\theta} \right)^2 = <\cos(\theta)>_J^2 \tag{24}$$

$$\Psi_B \cong <\cos(\theta)>_J^2 = \left(\frac{I_{Axial}}{I_{Beam}} \right)^2 \tag{25}$$

Off-axis cosine losses integrated in the numerator of Eq. (24) quantify the axial component of beam current that generates thrust. This formulation has been used in past analyses[24,51], and creates a method where the plume divergence vector loss is evaluated in a scalar form. The calculation of Ψ_B is complicated by the presence of charge exchange in the plume, which increases measured beam current at large angles from centerline and artificially increases divergence losses.

An effective plume divergence angle may be calculated as shown in Eq. (26). This angle is significantly less than the typically reported 95% divergence half-angle.

$$\lambda = \cos^{-1}\left(<\cos(\theta)>_J\right) = \cos^{-1}\left(\frac{I_{Axial}}{I_{Beam}}\right) \tag{26}$$

The ratio $\dot{m}(\theta)v(\theta)/J(\theta)$ introduced in Eq. (24) reveals the difference between momentum-weighted divergence and charge-weighted divergence. This ratio is evaluated in Appendix C for variations in mass utilization and ion species population. In Eq. (27), the ratio is evaluated at angular position θ and reduced to a function of Q and Φ_m.

$$\frac{\dot{m}(\theta)\bar{v}(\theta)}{J(\theta)} = \left(2V_a\frac{\mathcal{M}}{\mathcal{F}}\right)^{1/2}\Phi_m\left(\frac{\Phi_P}{\chi}\right)^{1/2}\left[1+\frac{y_0^2(1-\Phi_m)}{\chi}\right]^{1/2}\Bigg|_\theta \propto \Phi_m Q^{-1/2} \tag{27}$$

Spatial variation of the average ion charge and mass utilization in the plume is the primary source of discrepancy between momentum-weighted divergence and charge-weighted divergence. Significant variations in Q and Φ_m within the angular region of highest beam current will have the greatest effect on plume divergence calculations. However, these variations are negligible in typical Hall thruster and ion engine plumes. Variations in propellant efficiency and average ion acceleration potential in the plume may also result in disparities, but are secondary effects and not expected to fluctuate at the angular region of peak beam current.

E. Evaluating Exchange Parameters and Thruster Performance

Two experimental parameters, denoted E_1 and E_2, may be written using the preceding utilization efficiencies to isolate changes in performance due to processes related to thrust or discharge current. The parameters are formed in Eq. (28) such that the product of E_1 and E_2 is equal to anode thruster efficiency. Equations (29) and (30) show how these quantities are calculated based solely on telemetry and thrust measurements, and

provide insight about the relative magnitudes of the individual utilization efficiencies in the absence of plume measurements.

$$\eta_A = \left[\Phi_P \, \Psi_B (1-\beta) \chi\right] \left[\frac{(1-r)}{\chi}\right] = E_1 \, E_2 \tag{28}$$

$$E_1 = \Phi_P \, \Psi_B (1-\beta) \chi = \frac{\frac{1}{2}\left[\frac{T}{\dot{m}}\right]^2}{V_d \frac{\mathcal{F}}{\mathcal{M}}} \tag{29}$$

$$E_2 = \frac{(1-r)}{\chi} = \frac{\dot{m}}{I_d} \frac{\mathcal{F}}{\mathcal{M}} \tag{30}$$

For fixed thruster telemetry inputs V_d and $\dot{m}$, the dimensionless experimental parameter E_1 separates changes in anode efficiency directly to variations in thrust and E_2 isolates changes due to variations in discharge current. The quantity $E_1 \sim T^2$, and is a function of propellant efficiency, beam efficiency, voltage utilization, and χ. Experimental parameter E_1 relates the applied acceleration potential to dispersion and divergence of the jet. The quantity $E_2 \sim I_d^{-1}$, and is a function of current utilization and χ. Experimental parameter E_2 relates the input flow of mass to the total output flow of charge. The inverse of E_2 was used in the Soviet literature[52] as early as 1978 and termed the exchange parameter.[53,54] The naming convention used here describes the exchange of applied input parameters to operational thruster properties. Thus, E_1 is termed the voltage exchange parameter and E_2 is termed the mass exchange parameter. While ionization and acceleration processes are closely coupled, the form of the experimental parameters indicates that propellant efficiency, beam efficiency, and voltage utilization are principal in the formation of directed thrust. In the absence of diagnostics for the determination of plasma properties, these experimental parameter groups allow limits to be placed on acceptable values for the average charge, mass utilization, and plume divergence. [55,56]

The loss mechanisms that effect T/P and Isp are shown in Eq. (31) and (32) in terms of the experimental parameters E_1 and E_2 and in terms of the utilization efficiencies. These formulations indicate low current utilization and large χ will decrease T/P. Conversely, specific impulse is not directly affected by current utilization and increases for large χ. It is interesting to note the mass utilization in propellant efficiency and χ cancels in the formulation of T/P, which suggests the increased T/P at low discharge voltage is not directly affected by ionization losses.[57]

$$\frac{T}{P_{in}} = E_2\, E_1^{1/2} \left(\frac{2}{V_d} \frac{\mathscr{M}}{\mathscr{F}} \right)^{1/2} = (1-r)(1-\beta)^{1/2} \left(\frac{\Phi_P\, \Psi_B}{\chi} \right)^{1/2} \left(\frac{2}{V_d} \frac{\mathscr{M}}{\mathscr{F}} \right)^{1/2} \tag{31}$$

$$I_{sp}\, g = E_1^{1/2} \left(2V_d \frac{\mathscr{F}}{M} \right)^{1/2} = (1-\beta)^{1/2} \left(\chi\ \Phi_P\ \Psi_B \right)^{1/2} \left(2V_d \frac{\mathscr{F}}{M} \right)^{1/2} \tag{32}$$

The T/P formulation is similar to the one dimensional analysis used to estimate thrust of the SERT-II ion engines, which is equivalent to Eq. (31) when the term ($\Phi_P\ \Psi_B / \chi$) is unity.[58,59,60,61,62,63] An analogous expression was used to estimate thrust of the NSTAR ion engines on-board NASA's Deep Space 1 by including factors to estimate the effect of multiply charged ions and beam cosine losses.[64] These factors were similar those in the formulation of thrust by Masek *et al.* and are related to the ratio $(\Phi_P\ \Psi_B / \chi)^{1/2}$ for a bimodal ion population.[17] The formulations of T/P and Isp in Eq. (31) and (32) will be used in addition to the anode efficiency to evaluate the fidelity of plume measurements in evaluating thruster performance.

IV. Application to Experimental Results

A. Experimental Apparatus

The efficacy of the performance architecture is studied using experimental results from a nominal 6 kW Hall thruster in Chamber 3 at the Air Force Research Laboratory.[65] Operation of the laboratory model thruster with a center-mount cathode ranges from 105 V to 300 V with 10 mg/s Xe anode flow. Cathode flow fraction (CFF = cathode flow rate / anode flow rate) is increased for low discharge voltage operation to maintain stability and maximize total efficiency.

The study consists of thrust measurements and examination of the ion voltage distribution, plasma potential, ion species composition, and ion current density in the far-field plume. Facility effects on thrust and current density profiles are minimized by extrapolating measurements at several background pressures to zero pressure. This technique is commonly used to approximate thrust in the space environment from ground measurements, and was recently adapted to estimate current density profiles in the plume.[66] Faraday probe sweeps were executed in a 1 m hemispherical arc from 0° to 180°, and RPA measurements were taken at several angular positions in a 1 m hemispherical arc. The RPA most probable ion pass voltage was corrected with Langmuir probe plasma potential measurements less than 3 cm from the probe, which resulted in negligible variation in the most

probable ion acceleration potential over a large angular span. The ion species composition was evaluated from 1 m to 1.3 m downstream of the exit plane on channel centerline and current fractions were corrected for the loss of beam ions due to CEX collisions using the procedure outlined by Shastry.[67] Conclusions from a recent study of angularly resolved ExB probe spectra using this thruster model asserted that a single point channel centerline measurement was representative of species fractions the plume, and deviated from plume averaged results by less than 1.5% over a wide range of thruster operating conditions.[68] ExB and RPA results in the next section are not plume averaged, and variations are accounted for in the specified uncertainty. Further details concerning the facility, diagnostics, and measurement uncertainty are described elsewhere.[65]

B. Experimental Results and Analysis

Experimental results and measurement uncertainty are listed in Table 1 for constant 10 mg/s anode flow operation from 105 V to 300 V discharge. This set of thrust and plume measurements enable full characterization of the thruster utilization efficiencies and performance parameters.

Table 1: Thrust, Telemetry, and Far-field Plume Measurements of a 6 kW Laboratory Hall Thruster [65]

	105 V, 10 mg/s 16% CFF	**120 V, 10 mg/s 12% CFF**	**150 V, 10 mg/s 7% CFF**	**300 V, 10 mg/s 7% CFF**
V_d [V]	105 ± 0.05%	120 ± 0.05%	150 ± 0.05%	300 ± 0.05%
I_d [A]	9.8 ± 0.2%	9.5 ± 0.2%	9.1 ± 0.2%	8.8 ± 0.2%
$\dot{m}$ [mg/s]	10.0 ± 1%	10.0 ± 1%	10.0 ± 1%	10.0 ± 1%
T [mN]	87 ± 1%	92 ± 1%	112 ± 1%	184 ± 1%
Ω_1	0.91 ± 0.04	0.90 ± 0.04	0.86 ± 0.04	0.82 ± 0.04
Ω_2	0.09 ± 0.02	0.10 ± 0.02	0.10 ± 0.02	0.12 ± 0.02
Ω_3	0.0 ± 0.01	0.0 ± 0.01	0.04 ± 0.01	0.06 ± 0.01
V_a [V]	81 ± 8	92 ± 9	120 ± 9	266 ± 10
I_{Beam} [A]	7.1 ± 5%	6.9 ± 5%	7.1 ± 5%	7.4 ± 5%
I_{Axial} [A]	5.9 ± 5%	5.8 ± 5%	6.5 ± 5%	7.2 ± 5%

The uncertainty in thrust and plume measurements were propagated into calculations of plasma properties and utilization efficiencies. These values are calculated using standard error propagation techniques (% Error $= \sqrt{(\%\text{Error}_1)^2 + (\%\text{Error}_2)^2 + \ldots}$) for independent measurements. Uncertainty in calculations with correlated terms is

conservatively estimated. Correlated terms include the axial and total ion beam current from a Faraday probe and the ion current fractions from the ExB probe.

Specific impulse, T/P, and anode efficiency based on plume measurements are compared to the values determined by thrust measurements in Fig. 1. Agreement between the performance parameters is within the error bars for all operating conditions, with the greatest difference occurring at 105 V and 120 V. The consistent agreement between thrust measurements and plume measurements indicates the efficiency architecture is accurately capturing the thruster performance characteristics. Comparison of the interrelated T/P and Isp terms at each operating condition support the measurement validity and corroborate the formulation of loss mechanisms in Eq. (31) and (32).

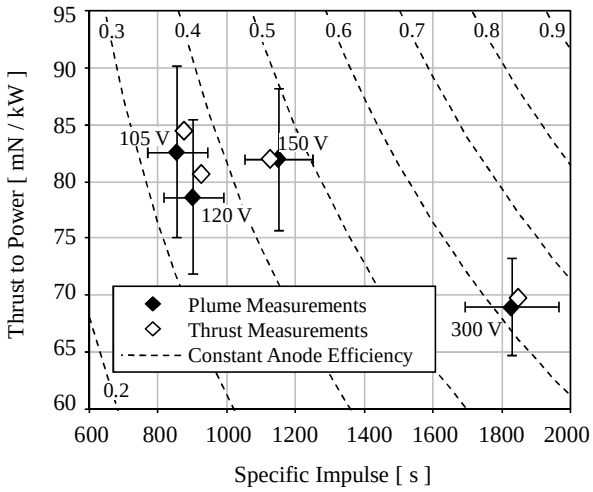

Fig. 1 Thrust to power ratio as a function of specific impulse with lines of constant anode efficiency for a 6 kW laboratory Hall thruster ranging from 105 V to 300 V at 10 mg/s operation.

Anode thruster efficiency is separated into utilization efficiencies in Fig. 2. Reduced anode efficiency at low discharge voltage is primarily due to increased beam divergence and increased energy losses. Beam efficiency decreases from 0.94 at 300 V to 0.69 at 105 V, which corresponds to an increase in divergence half-angle from 14° to 34°. The decline in energy efficiency with discharge voltage is the dominant loss mechanism during low voltage operation. Propellant efficiency varies by less than 2% over the range of operation, and shows a slight increase at the lowest discharge voltages. This effect is studied by decomposing propellant efficiency into mass, charge, and neutral-gain utilization efficiencies in Fig. 3.

The charge utilization decreases at higher discharge voltage due to the production of multiply charged ions, which is consistent with past investigations.[43,68] Increased mass utilization at low voltage is most likely caused by additional ionization as a consequence of the increased CFF, and is responsible for the increased propellant efficiency at low voltage. Variations in neutral-gain utilization due to neutral speed are quantified in Appendix B. The neutral speed is conservatively estimated at 200 m/s based on LIF studies of this thruster model at the University of Michigan.[47]

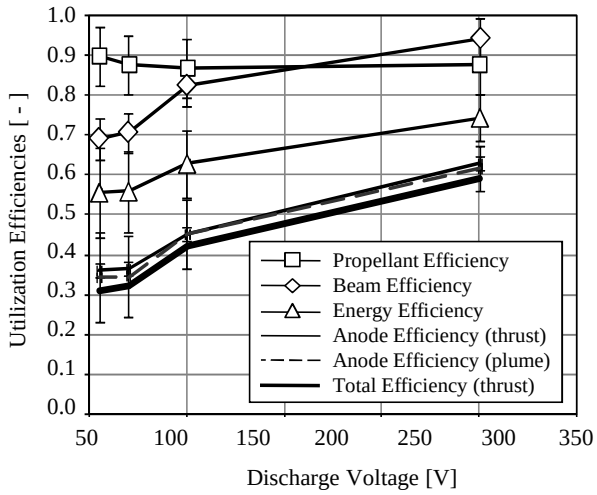

Fig. 2 Anode efficiency and utilization efficiencies as a function of discharge voltage for a 6 kW laboratory Hall thruster ranging from 105 V to 300 V at 10 mg/s operation.

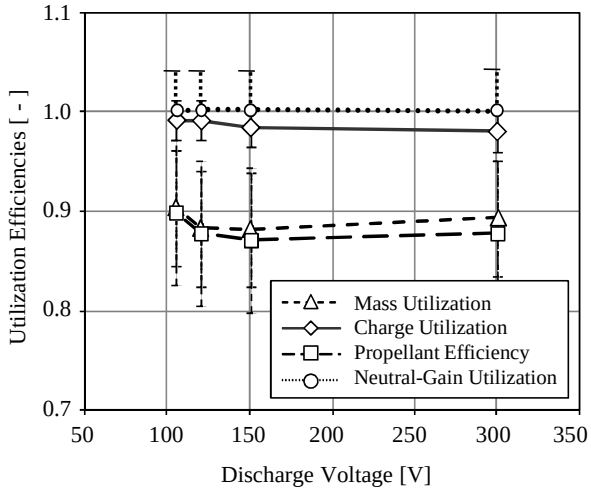

Fig. 3 Propellant efficiency, mass utilization, charge utilization, and neutral-gain utilization as a function of discharge voltage for a 6 kW laboratory Hall thruster ranging from 105 V to 300 V at 10 mg/s operation.

Losses in energy efficiency are divided into current utilization and voltage utilization in Fig. 4. At low voltage, the ionization cost becomes a larger faction of the applied anode potential. The decrease in voltage utilization is approximately equal to the fractional increase of the xenon ionization potential relative to the thruster discharge voltage (12 eV / V_d). The fraction of electron current to the anode is the dominant loss mechanism in energy efficiency, and is magnified during low voltage operation.

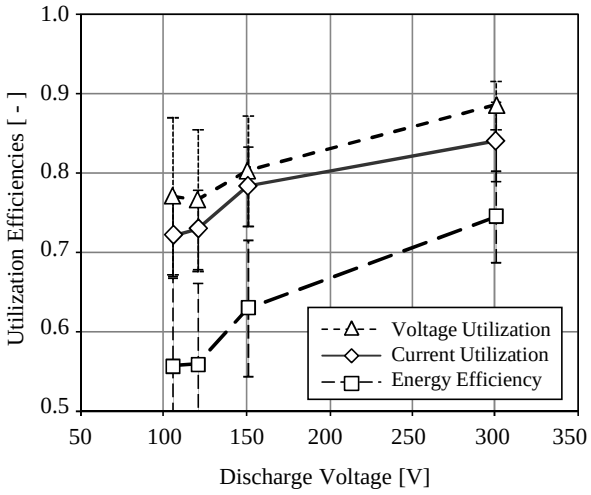

Fig. 4 Energy efficiency, voltage utilization, and current utilization as a function of discharge voltage for a 6 kW laboratory Hall thruster ranging from 105 V to 300 V at 10 mg/s operation.

In Fig. 5, the fraction of recycled electron current is compared to the minimum electron current to the anode necessary to sustain ionization. As thruster power is decreased for constant mass flow operation, the measured anode electron current fraction increased. The increase in r was larger than the increase in r_{min}, and highlights a significant loss mechanism associated with low voltage Hall thruster operation. The decrease in r_{min} with increased discharge power is expected for higher discharge voltage operation from Eq. (22).

Total power losses as a function of discharge power are estimated in Fig. 6. The minimum power loss to sustain ionization, P_{min} ~120 W, is nearly constant from 1000 W to 2600 W discharge power. Total Joule heating from cathode electrons, $P_d\, r_{min}$, is relatively constant below 150 V discharge, and increases by 50% to 300 W during 300 V operation. This increased Joule heating from recycled electrons with increased discharge power indicates excessive losses to the channel walls and plasma excitation processes. The total power loss in the thruster is

estimated using energy efficiency. It is important to note these power losses do not account for the spread in most probable ion potential or variations in the plume, which introduce significant error in the estimates. Further isolation of energy loss mechanisms are unfeasible with plume measurements, and require numerical simulations to determine the effects of wall collisions, radiation, excitation and relaxation processes.

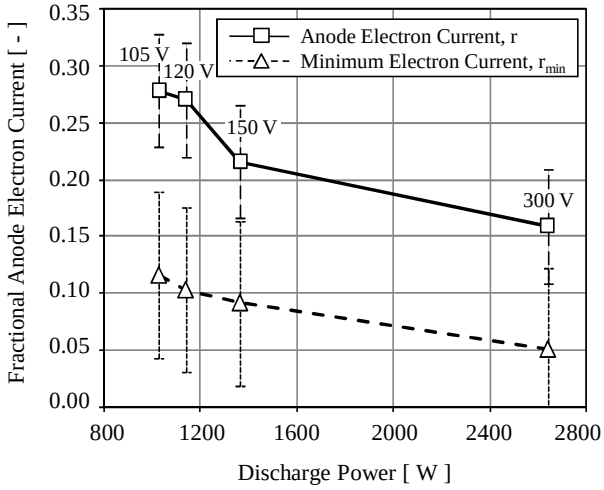

Fig. 5 Fractional anode electron current and minimum anode electron current as a function of discharge power for a 6 kW laboratory Hall thruster ranging from 105 V to 300 V at 10 mg/s operation.

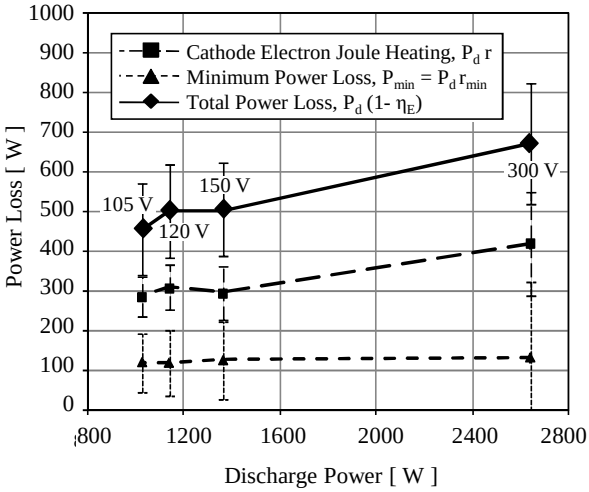

Fig. 6 Power losses as a function of discharge power for a 6 kW laboratory Hall thruster ranging from 105 V to 300 V at 10 mg/s operation.

V. Summary

The separation of scalar thrust into mass-weighted and momentum-weighted terms enabled factorization of anode efficiency into the product of (1) energy efficiency, (2) propellant efficiency, and (3) beam efficiency. The analysis decomposed anode efficiency from first principles, and formulated the relationship such that losses associated with energy conversion are analyzed separately from losses associated with dispersion of the jet VDF and beam divergence. The effects of multiply charged ions are included, and the neutral-gain utilization is introduced to account for the neutral speed. The momentum-weighted divergence loss term ($<\cos(\theta)>^2_{mv}$) contains all jet vector losses, and differences from the current-weighted divergence was characterized. The proposed analysis is compared to past performance methodologies, with similarities to previous architectures formulated by Masek *et al*. in the ion engine community[17], Belan *et al.* from the Kharkov Aviation Institute[24], and a contemporary methodology by Hofer.[43,50]

A case study was presented with experimental performance and far-field plume measurements for a 6 kW laboratory Hall thruster. Comparison of calculated anode efficiency, T/P, and Isp for constant anode flow operation from 105 V to 300 V showed good agreement between the analytical model and plume diagnostics. The performance methodology highlights low current utilization and beam divergence as the primary loss mechanisms during low voltage operation. Current utilization can never be unity due to a finite flow of electrons that are recycled to the anode to sustain ionization processes. Power losses and Joule heating processes are estimated for each operating condition. The minimum power loss to sustain ionization showed minimal variation with increasing discharge power for constant anode mass flow operation. For increasing voltage utilization with discharge voltage, the increasing power losses during high voltage operation are the result of additional wall collisions, radiation, excitation and relaxation processes within the discharge channel.

Acknowledgements

The authors acknowledge numerous insightful discussions with Justin Koo, Brian Beal, Bill Hargus, Michelle Scharfe, Bryan Reid, and James Haas that contributed to development of the ideas and concepts presented in this paper.

APPENDIX A: Definitions of Mass-weighted and Momentum-weighted Quantities

In Eq. (2), the steady state equation for axisymmetric thrust directed along thruster centerline was factored into the product of mass flow, mass-weighted average velocity, and momentum-weighted average divergence using the definitions shown in Eq. (A-1), (A-2), (A-3), and (A-4).

Hemispherical integration of mass flow rate throughout the plume at constant radius in Eq. (A-1) is equal to the total mass flow rate supplied to the anode. Propellant flow exiting the cathode has a negligible effect on thrust since it is composed primarily of neutrals. Thus, cathode flow is considered a parasitic loss and is not included in this definition.

$$\dot{m} = 2\pi R^2 \int_0^{\pi/2} \dot{m}(\theta)\sin(\theta)\,d\theta \tag{A-1}$$

The average velocity vector, $\overline{\mathbf{v}}$, is defined in Eq. (A-2) as the integral of the VDF over all velocity space at for an axisymmetric plume at angular position θ and radius R. The radial propellant velocity component in spherical coordinates, $\overline{v}$, is formulated in Eq. (A-3) and radial ion velocity component, $\overline{v_i}$, is formulated in Eq. (A-4) using ion flow fractions. This is the dominant velocity component for ions originating from the thruster discharge, and other velocity components in the plume are negligible. Squared ion and propellant radial velocity terms are found using analogous expressions.

$$\overline{\mathbf{v}} = \iiint \mathbf{v}\, f(\mathbf{v})\,d\mathbf{v} \Big/ \iiint f(\mathbf{v})\,d\mathbf{v} \tag{A-2}$$

$$\overline{v} = \sum_{j=0} \frac{\dot{m}_j}{\dot{m}} v_j \tag{A-3}$$

$$\overline{v_i} = \sum_{j=1} \frac{\dot{m}_j}{\dot{m}_i} v_j = \sum_{j=1} f_j^* v_j \tag{A-4}$$

The mass-weighted average radial velocity component for an axisymmetric plume is defined in Eq. (A-5) and simplified using Eq. (A-1). The momentum-weighted average cosine is defined in Eq. (A-6) and simplified using Eq. (A-5). The definition of thrust in Eq. (2) is naturally produced through the relation of mass-weighted and momentum-weighted terms in Eq. (A-6). This formulation of thrust sets the foundation for the Hall thruster efficiency architecture outlined the paper.

$$< \bar{v} >_m = \frac{2\pi R^2 \int_0^{\pi/2} \dot{m}(\theta)\, \bar{v}(\theta) \sin(\theta)\, d\theta}{2\pi R^2 \int_0^{\pi/2} \dot{m}(\theta) \sin(\theta)\, d\theta} = \frac{2\pi R^2 \int_0^{\pi/2} \dot{m}(\theta)\, \bar{v}(\theta) \sin(\theta)\, d\theta}{\dot{m}} \tag{A-5}$$

$$< \cos(\theta) >_{mv} = \frac{2\pi R^2 \int_0^{\pi/2} \dot{m}(\theta)\, \bar{v}(\theta) \cos(\theta) \sin(\theta)\, d\theta}{2\pi R^2 \int_0^{\pi/2} \dot{m}(\theta)\, \bar{v}(\theta) \sin(\theta)\, d\theta} = \frac{2\pi R^2 \int_0^{\pi/2} \dot{m}(\theta)\, \bar{v}(\theta) \cos(\theta) \sin(\theta)\, d\theta}{\dot{m} < \bar{v} >_m} \tag{A-6}$$

All quantities are assumed steady state and evaluated at constant radius from the exit plane, such that the quantities to be integrated have units of sr^{-1}. For hemispherical integration about a point source, the measurement distance must be multiple thruster diameters downstream of the exit. The definitions in Eq. (A-1) through (A-6) do not account for dispersion of the jet due to scattering and charge exchange ions in the plume. These processes will have a different effect depending on the diagnostic, facility, background pressure, and distance from the thruster. To this point, an axisymmetic plume with radial particle velocity and negligible facility effects are the only approximations required.

APPENDIX B: Formulation of Neutral-Gain Utilization in Propellant Efficiency

Propellant efficiency characterizes dispersion of the VDF and is a measure of the jet momentum relative to the jet kinetic energy. In Eq. (B-1) and (B-2), the second term in brackets in Eq. (7) is decomposed into the product of mass utilization and neutral-gain utilization.

$$\frac{\left[< \overline{v} >_m \Big/ < \overline{v_i} >_m \right]^2}{< \overline{v^2} >_m \Big/ < \overline{v_i^2} >_m} = \frac{\left[\sum_{j=0} \left(\frac{\dot{m}_j}{\dot{m}} v_j \right) \Big/ \sum_{j=1} \left(\frac{\dot{m}_j}{\dot{m}_i} v_j \right) \right]^2}{\sum_{j=0} \left(\frac{\dot{m}_j}{\dot{m}} v_j^2 \right) \Big/ \sum_{j=1} \left(\frac{\dot{m}_j}{\dot{m}_i} v_j^2 \right)} = \frac{\left[\Phi_m \sum_{j=0} \left(f_j^* y_j \right) \Big/ \sum_{j=1} \left(f_j^* y_j \right) \right]^2}{\Phi_m \sum_{j=0} \left(f_j^* y_j^2 \right) \Big/ \sum_{j=1} \left(f_j^* y_j^2 \right)} \tag{B-1}$$

$$\frac{\left[< \overline{v} >_m \Big/ < \overline{v_i} >_m \right]^2}{< \overline{v^2} >_m \Big/ < \overline{v_i^2} >_m} = \Phi_m \frac{\left[1 + \frac{y_0 \left(1 - \Phi_m \right)}{\Phi_m \sqrt{\Phi_q Q}} \right]^2}{\left[1 + \frac{y_0^2 \left(1 - \Phi_m \right)}{\Phi_m Q} \right]} = \Phi_m \Phi_{N\text{-}G} \tag{B-2}$$

The neutral-gain utilization is defined in Eq. (B-3), and is always greater than unity. The approximation in Eq. (12) is formulated by neglecting second order terms with y_0, and shows $\Phi_{N\text{-}G}$ is primarily a function of the neutral speed and mass utilization. Effects that increase the neutral-gain utilization result in detrimental losses to other utilization efficiencies. Ideal thruster operation would correspond to unity neutral-gain for 100% ionization or zero neutral speed for infinite neutral residence time in the channel.

$$\Phi_{N\text{-}G} = \frac{\left[1 + \frac{y_0 \left(1 - \Phi_m \right)}{\Phi_m \sqrt{\Phi_q Q}} \right]^2}{\left[1 + \frac{y_0^2 \left(1 - \Phi_m \right)}{\Phi_m Q} \right]} \approx 1 + \frac{2 y_0 \left(1 - \Phi_m \right)}{\Phi_m \sqrt{\Phi_q Q}} \tag{B-3}$$

The small gain in efficiency due to the neutral speed is generally neglected. Neutral-gain utilization is plotted in Fig. (B-1) for Q=1, and is shown to increase with reduced mass utilization and large neutral speed. Thrusters with a high neutral thermal speed or large axial injection speed may exhibit neutral-gain utilization of 1.01 to 1.02. In Fig. (B-2), the neutral-gain utilization is shown for the ion species composition of the 6 kW laboratory thruster studied in Section IV. Mass utilization of Hall thrusters typically ranges from 0.80 to 0.90 for nominal operation. For estimates of $y_0 \approx 0.02$,[47] the neutral-gain utilization is approximately 1.005 when mass utilization is 0.90. The neutral-gain is expected to be larger for low discharge voltage, high power operation where the value of y_0 is increased and ionization is reduced.

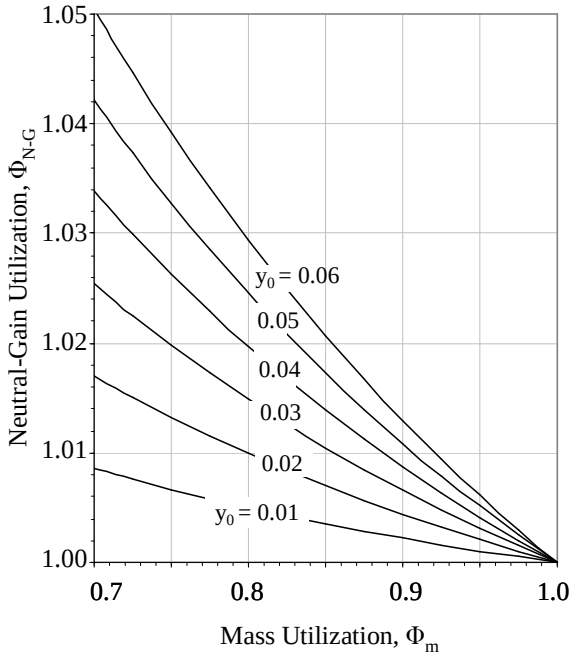

Fig. B-1 Neutral-gain utilization as a function of mass utilization with variations in reduced neutral speed from y_0=0.01 to y_0=0.06 for Q=1.

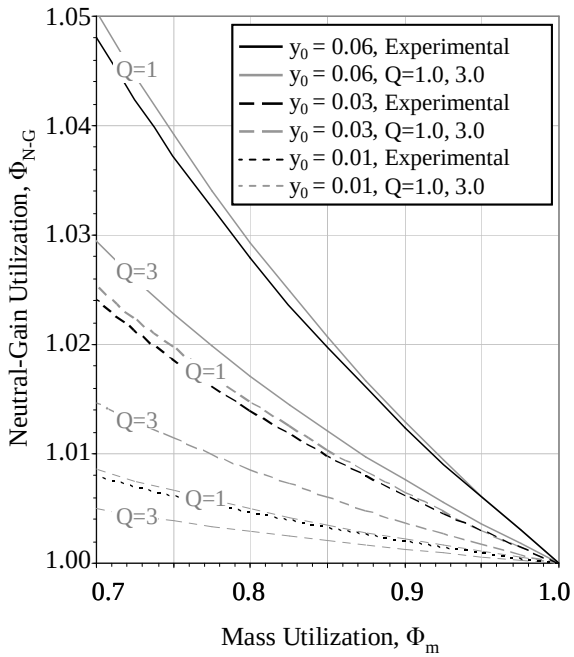

Fig. B-2 Neutral-gain utilization for the ion species composition of the 6 kW laboratory Hall thruster during 300 V, 10 mg/s operation as a function of mass utilization for y_0=0.01, 0.03, and 0.06. Neutral-gain of the experimental ion composition is bounded by lines of constant Q=1 and Q=3, which are limiting cases for a trimodal ion population.

APPENDIX C: Comparison of Momentum-weighted and Charge-weighted Plume Divergence

The momentum-weighted average divergence is approximated as the charge-weighted average divergence in Eq. (24), which enables calculation of off-axis cosine losses using the ratio of the axial component of beam current to total beam current as measured by a Faraday probe.

Analysis of the ratio $\dot{m}(\theta)v(\theta)/J(\theta)$ introduced in Eq. (24) characterizes the properties that cause differences between momentum-weighted divergence and charge-weighted divergence. The ratio is evaluated at angular position θ In Eq. (C-1). Each particle species is approximated with a delta function velocity distribution and velocity ratios are calculated for the idealized case of ion creation at the same location. The ratio $\dot{m}(\theta)v(\theta)/J(\theta)$ is characterized using the dimensionless quantity γ, which describes differences associated with ionization fraction and ion species population. The term γ is shown as a function of Φ_m, Φ_P, χ, and y_0 in Eq. (C-2).

$$\left.\frac{\dot{m}(\theta)\bar{v}(\theta)}{J(\theta)} = \frac{\sum_{j=0}\dot{m}_j v_j}{\sum_{j=1}\dot{m}_j Z_j \left(\mathscr{F}/\mathscr{M}\right)}\right|_\theta = \left.\frac{\dot{m}\Phi_m |v_1| \sum_{j=0} f_j^* y_j}{\dot{m}\Phi_m Q \left(\mathscr{F}/\mathscr{M}\right)}\right|_\theta = \left.\left(2V_a \frac{\mathscr{M}}{\mathscr{F}}\right)^{1/2} \gamma\right|_\theta \tag{C-1}$$

$$\gamma = \frac{\sum_{j=0} f_j^* \sqrt{Z_j}}{Q} = \Phi_m \left(\frac{\Phi_P}{\chi}\right)^{1/2} \left[1 + \frac{y_0^2 (1-\Phi_m)}{\chi}\right]^{1/2} \approx \Phi_m Q^{-1/2} \tag{C-2}$$

The term inside the brackets of Eq. (C-2) is near unity for $y_0 \approx 0.02$,[47] and variations in the neutral speed ratio have negligible effect on γ. In Figure C-1, γ is shown for mass utilization ranging from 0.6 to 1.0 and y_0=0.02. The ratio is bounded for a trimodal ion population, and is shown to be primarily a function of mass utilization and average charge.

Variations in the magnitude of Φ_m and Q alter γ, but the angular location of these variations is the dominant factor causing differences between momentum-weighted divergence and charge-weighted divergence. This effect is illustrated in Figure C-2, which shows a representative distribution of current density and beam current as a function of angular position for the 6 kW laboratory Hall thruster from Section IV operating at 300 V. The location of peak beam current in the plume is approximately 8 degrees from thruster centerline, and variations in Φ_m and Q within the angular range of full width half maximum (FWHM) will have the greatest effect on divergence. For the beam current in Figure C-2, this range is approximately ±3 to ±21 degrees. Near and far-field plume measurements of the the 6 kW Hall thruster[68], the SPT-100[48,69] and the BHT-200[70] Hall thruster found that the ion species populations did not significantly change within ±15 degrees from thruster centerline, and the fraction of Xe^{+2} increased sharply

by approximately 5% at ±20 degrees. These changes in ion species composition have a negligible effect on the value of $\langle\cos(\theta)\rangle_{mv}$, thus enabling the approximation of equivalence between momentum-weighted divergence and charge-weighted plume divergence as measured with a Faraday probe.

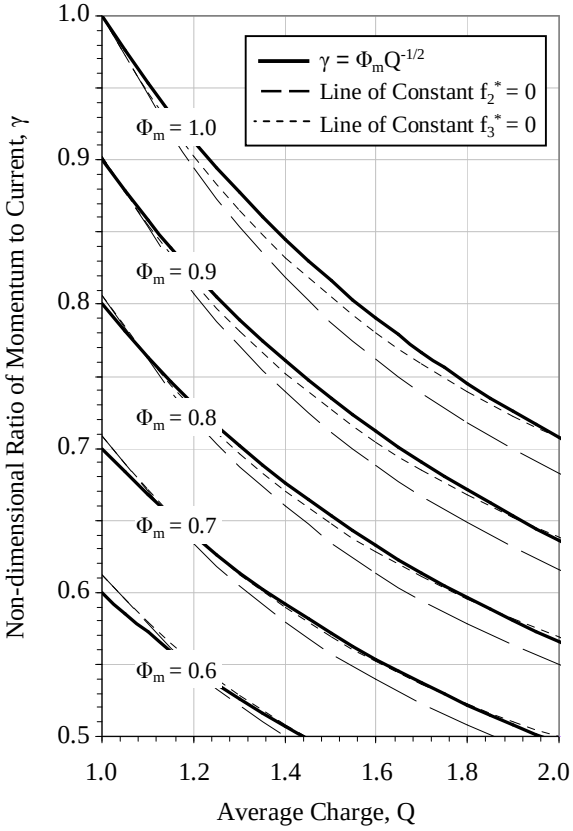

Fig. C-1 Variation in γ due to mass utilization and ion species composition. Mass utilization manifolds are shown for Φ_m = 1.0, 0.9, 0.8, 0.7, and 0.6. Lines of constant f_2^*=0 and f_3^*=0 bound γ for a trimodal ion population, and are compared with the approximation $\gamma \approx \Phi_m Q^{-1/2}$.

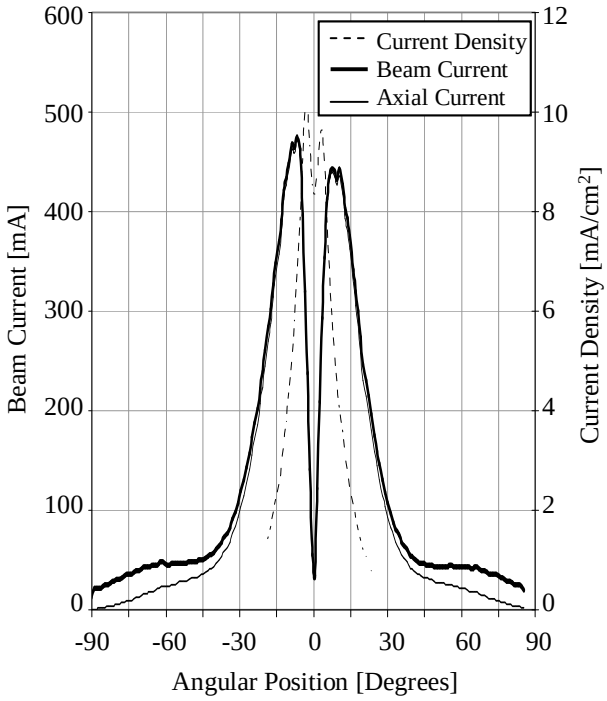

Fig. C-2 Representative distribution of beam current and current density at 1 meter radius as a function of angular position in the plume of a nominal 6 kW laboratory Hall thruster operating at 300 V, 10 mg/s from Section IV.

REFERENCES

[1] Semenkin, A., Kim, V., Gorshkov, O., Jankovsky, R., "Development of electric propulsion standards – current status and further activity," Proceedings of the 27th International Electric Propulsion Conference, Pasadena, CA, 15-19 October, 2001, Paper No. IEPC-2001-70.

[2] Morozov, A. I., "About Plasma Acceleration by Magnetic Fields," *Journal of Experimental and Theoretical Physics*, Vol. 32, N2, pp. 305, 1957 (In Russian).

[3] Yushmanov, E. E., *Radial Distribution of the Potential in Cylindrical Trap with Magnetron Ion Injection, In Book: Plasma Physics and the Problem of Controlled Fusion*, M. A. Leontovich, Ed. Moscow, USSR: USSR Academy of Science, 1958, vol. 4, (In Russian).

[4] Zharinov, A. V., "Electric Double Layer in Strong Magnetic Field," Kurchatov Inst. Rep., Moscow, USSR, 1961 (In Russian).

[5] Lary, E.C., Meyerand, R. G. Jr., Salz, F., "Ion Acceleration in a gyro-dominated neutral plasma: Theory and experiment," *Bulletin of the American Physical Society*, Vol. 7, pg. 441, July 1962.

[6] Seikel, G. R., Reshotko, E., "Hall-current Ion Accelerator," *Bulletin of the American Physical Society*, Vol. 7, pg. 414, July 1962.

[7] Janes, G. S., Dotson, J., Wilson, T., "Electrostatic Acceleration of Neutral Plasmas – Momentum Transfer Through Magnetic Fields," Proceedings of the Third Symposium on Advanced Propulsion Concepts (Gordon and Breach Science Publishers, Inc., New York, 1963), pg. 153 – 175.

[8] Brown, C. O., Pinsley, E. A., "Further Experimental Investigations of a Cesium Hall-Current Accelerator," *AIAA Journal*, Vol. 3, No. 5, 1965, pp. 853-859.

[9] Morozov, A. I., "Investigation of the stationary electromagnetic plasma acceleration" – Doctoral Thesis, Institute of Atomic Energy named after I. V. Kourchatov, Moscow, 1965 (In Russian).

[10] Janes, G. S., Lowder, R. S., "Anomalous Electron Diffusion and Ion Acceleration in a Low-Density Plasma", *Physics of Fluids*, Vol. 9, No. 6, 1966.

[11] Zharinov, A. V., Popov, Y. S., "Acceleration of plasma by a closed Hall current," *Soviet Physics – Technical Physics*, Vol. 12, No. 2, August 1967, p. 208-211 (In Russian).

[12] Morozov, A. I., "Effect of Near-wall Conductivity in Magnetized Plasma," *Journal of Applied Math Technical Physics*, Vol. 3, pg. 19-22, 1968 (In Russian).

[13] Kaufman, H. R., "Technology of Closed-Drift Thrusters," *AIAA Journal*, Vol. 23, No. 1, 1985, pp. 78-87.
[14] Zhurin, V. V., Kaufman, H. R., and Robinson, R. S., "Physics of closed drift thrusters," *Plasma Sources Sci. Technol*., Vol. 8, 1999, pp. R1-R20.
[15] Morozov, A. I., "The Conceptual Development of Stationary Plasma Thrusteres", *Plasma Physics Reports*, Vol. 29, No. 3, pg. 235-250, 2003 (Translated from Fizika Plazmy, Vol. 29, No. 3, pg. 261-276, 2003)
[16] Kim, V., "History of the Hall Thrusters Development in USSR", Proceedings of the 30th International Electric Propulsion Conference, Florence, Italy, 17-20 September 2007, Paper No. IEPC-2007-142.
[17] Masek, T. D., Ward, J. W., Kami, S., "Primary Electric Propulsion Thrust Subsystem Definition," AIAA 11th Electric Propulsion Conference and Exhibit, 19-21 March 1975, New Orleans, LA, Paper No. AIAA 75-405.
[18] Brophy, J. R., "Stationary Plasma Thruster Evaluation in Russia", JPL Publication 92-4, NASA-CR-192823, March 15, 1992.
[19] Garner, C. E., Brophy, J. R., Polk, J. E., Semenkin, S., Garkusha, V., Tverdokhlebov, S., Marrese, C., "Experimental Evaluation of Russian Anode Layer Thrusters," 30th AIAA/ASME/SAE/ASEE Joint Propulsion Conference, 27-29 June, 1994, Indianapolis, IN, Paper No. AIAA 1994-3010.
[20] Meyer, R. M., Manzella, D. H., "SPT Thruster Plume Characteristics", Proceedings of the 23rd International Electric Propulsion Conference, Seattle, WA, 13-16 September 1993, IEPC-93-096.
[21] Sankovic, J. M., Hamley, J. A., Haag, T. W., "Performance Evaluation of the Russian SPT-100 Thruster at NASA LeRC", IEPC-93-094, Proceedings of the 23rd International Electric Propulsion Conference, Seattle, WA, 13-16 September 1993, Paper No. IEPC-93-094.
[22] Garner, C. E., Polk, J. E., Goodfellow, K. D., Brophy, J. R., "Performance Evaluation on Life Testing of the SPT-100," Proceedings of the 23rd International Electric Propulsion Conference, Seattle, WA, 13-16 September 1993, Paper No. IEPC-93-091.
[23] King, L. B., Gallimore, A. D., Marrese, C. M., "Transport-Property Measurements in the Plume of an SPT-100 Hall Thruster," *Journal of Propulsion and Power*, Vol. 14, No. 3, 1998, pg. 327-335.
[24] Belan, N. V., Kim, V. P, Oransky, A. I., Tikhonov, V. B., *Stationary Plasma Engines*, Khar'kov Karh'kovskiy Aviatsionnyy Institut, 1989, pp. 164 - 166. (in Russian)
[25] Bugrova, A. I., Kim, V. P, Maslennikov, N. A., Morozov, A. I., "Physical Properties and Characteristics of Stationary Plasma Thrusters with Closed Electron Drift", Proceedings of the 22nd International Electric Propulsion Conference, Viareggio, Italy, 1991, Paper No. IEPC 91-079.
[26] Kim, V., "Main Physical Features and Processes Determining the Performance of Stationary Plasma Thrusters", *Journal of Propulsion and Power*, Vol. 14, No. 5, September – October, 1998.
[27] Morozov, A. I., Bugrova, A. I., Desyatskov, A. V., Ermakov, Y. A., Kozintseva, M. V., Lipatov, A. S., Pushkin, A. A., Khartchevnikov, V. K., Churbanov, D. V., "ATON-Thruster Plasma Accelerator," *Plasma Physics Reports*, Vol. 23, No. 7, pp. 587-597, 1997 (Translated from Fizika Plazmy, Vol. 23, No. 7, pg. 635-645, 1997)
[28] Bugrova, A. I., Lipatov, A. S., Morozov, A. I., Baranov, S. V., "Effect of the Ratio of Differently Charged Ions on the Integral Parameters of Stationary Plasma Thrusters of the ATON Type," *Technical Physics Letters*, Vol. 31, No. 11, pp. 943-946, 2005 (Translated from Pis 'ma v Zhurnal Tekhnicheskoi Fiziki, Vol. 31, No. 21, pg. 87-94, 2005)
[29] Bouchoule, A., Boeuf, J. P., Heron, A., Duchemin, O., "Physical Investigations and Developments of Hall Plasma Thrusters", *Plasma Physics and Controlled Fusion*, 46 (2004), B407-B421.
[30] Grishin, S. D., Leskov, L. V., *Electrical Rocket Engines of Space Vehicles*, Publishing House "Mashinostroyeniye", Moscow, 1989, pp. 12.
[31] Raitses, Y., Ashkenazy, J., and Guelman, M., "Propellant Utilization in Hall Thrusters," *Journal of Propulsion and Power*, Vol. 14, No. 2, 1998, pp. 247-253.
[32] Raitses, Y., Fisch, N. J., "Parametric Investigations of a Nonconventional Hall Thruster," *Physics of Plasmas*, Vol. 8, No. 5, pg. 2579-2586, 2001.
[33] Ross, Jerry L., and King, Lyon B., "Ionization efficiency in electric propulsion devices," Proceedings of the 30th International Electric Propulsion Conference, Florence, Italy, 17-20 September 2007, Paper No. IEPC-2007-260.
[34] Sasoh, A., "Generalized Hall Acceleration," *Journal of Propulsion and Power*, Vol. 10, No. 2, 1994, pp. 251-254.
[35] Bober, A., "Numerical Analysis of Hall Thruster Firing Tests," *Journal of Propulsion and Power*, Vol. 23, No. 3, May-June 2007, pp. 537-543.
[36] Linnell, J. A., Gallimore, A. D., "Efficiency Analysis of a Hall Thruster Operating with Krypton and Xenon," *Journal of Propulsion and Power*, Vol. 22, No. 6, 2006, pg. 1402-1418.
[37] Fife, J. M., Martinez-Sanchez, M., "Two-Dimensional Hybrid Particle-In-Cell Modeling of Hall Thrusters," IEPC-95-240, Proceedings of the 24th International Electric Propulsion Conference, Moscow, Russia, 19-23 September 1995.
[38] Hruby, V., Monheiser, J., Pote, B., Rostler, P., Kolencik, J., and Freeman, C., "Development of low power Hall thrusters," 30th Plasmadynamics and Lasers Conference, 28 June – 1 July, 1999, Norfolk, VA, Paper No. AIAA 1999-3534.
[39] Jameson, K. K., Goebel, D. M., Hofer, R. R., Watkins, R. M., "Cathode coupling in Hall Thrusters," Proceedings of the 30th International Electric Propulsion Conference, Florence, Italy, 17-20 September 2007, Paper No. IEPC-2007-278.
[40] Hofer, R. R., Haas, J. M., Gallimore, A. D., "Ion Voltage Diagnostics in the Far-Field Plume of a High-Specific Impulse Hall Thruster," 39th AIAA/ASME/SAE/ASEE Joint Propulsion Conference and Exhibit, 20-23 July 2003, Huntsville, AL, Paper No. AIAA-2003-4556.

[41] Komurasaki, K., Arakawa, Y., "Hall Current Ion-Thruster Performance," *Journal of Propulsion and Power*, Vol. 8, No. 6, 1992, pp. 1212-1216.
[42] Ahedo, E., Gallardo, J. M., Martinez-Sanchez, M., "Model of the Plasma Discharge in a Hall Thruster with Heat Conduction," *Physics of Plasmas*, Vol. 9, No. 9, pg. 4061-4070, 2002.
[43] Hofer, R. R., and Gallimore, A.D., "High-specific impulse Hall Thrusters, Part 2: Efficiency Analysis," *Journal of Propulsion and Power*, Vol. 22, No. 4, 2006, pp. 732-740.
[44] Hofer, R. R., Katz, I., Mikellides, I. G., Goebel, D. M., Jameson, K. K., Sullivan, R. M., Johnson, L. K., "Efficacy of Electron Mobility Models in Hybrid-PIC Hall Thruster Simulations," 44th AIAA/ASME/SAE/ASEE Joint Propulsion Conference and Exhibit, 21-23 July 2008, Hartford, CT, Paper No. AIAA-2008-4924.
[45] Chavers, G., Chang-Diaz, F., Breizman, Boris, Bengston, R., "Momentum Flux Measurements Using an Impact Thrust Stand," 46th APS Annual Meeting of the Division of Plasma Physics, 15-19 November 2004, Savannah, GA, Meeting ID: DPP04.
[46] Hargus, W. A. Jr., Cappelli, M. A., "Interior and Exterior Laser-Induced Fluorescence and Plasma Measurements within a Hall Thruster," *Journal of Propulsion and Power*, Vol. 18, No. 1, 2002, pp. 159-168.
[47] Smith, T. B., Huang, W., Reid, B. M., Gallimore, A. D., "Near-field Laser-Induced Fluorescence Velocimetry of Neutral Xenon in a 6 kW Hall Thruster Plume," Proceedings of the 30th International Electric Propulsion Conference, Florence, Italy, 17-20 September 2007, Paper No. IEPC-2007-252.
[48] Kim, S. W., Gallimore, A. D., "Plume Study of a 1.35-kW SPT-100 Using an ExB Probe," *Journal of Spacecraft and Rockets*, Vol. 39, No. 6, 2002, pp. 904-909.
[49] King, L. B., "Transport-property and mass spectral measurements in the exhaust plume of a Hall effect space propulsion system," PhD Dissertation, University of Michigan, Ann Arbor, MI, 1998.
[50] Hofer, R. R., "Development and Characterization of High-Efficiency, High Specific Impulse Xenon Hall Thrusters," PhD Dissertation, University of Michigan, Ann Arbor, Michigan. Published as NASA/CR-2004-213099, 2004.
[51] Goebel, D. M., Katz, I., *Fundamentals of Electric Propulsion: Ion and Hall Thrusters*. (John Wiley & Sons, New York, 2007).
[52] Morozov, A. I., Physical Principles of Cosmic Electric Propulsion Engines, Moscow: Atomizdat, 1978.
[53] Morozov, A. I., Balebanov, V. M., Bugrova, A. I., Lipatov, A. S., Khartchevnikov, V. K., "ATON-Thruster Plasma Accelerator," 4th All-Russian Seminar on Problems of Theoretical and Applied Electron Optics, Proceedings of SPIE, Vol. 4187, 2000.
[54] Bugrova, A. I., Lipatov, A. S., Morozov, A. I., Churbanov, D. V., "On Similarity Criterion for Plasma Accelerators of the Stationary Plasma Thruster Type," *Technical Physics Letters*, Vol. 28, No. 10, pp. 821-823, 2002 (Translated from Pis 'ma v Zhurnal Tekhnicheskoi Fiziki, Vol. 28, No. 19, pg. 56-61, 2002)
[55] Larson, C. William, Brown, Daniel L., and Hargus, William A. Jr., "Thrust efficiency, energy efficiency and the role of the VDF in Hall thruster performance analysis," 43rd AIAA/ASME/SAE/ASEE Joint Propulsion Conference and Exhibit, 8-11 July, 2007, Cincinnati, OH, Paper No. AIAA 2007-5270.
[56] Brown, Daniel L., Larson, C. William, Haas, James M., and Gallimore, Alec D., "Analytical extraction of plasma properties using a Hall thruster efficiency architecture," Proceedings of the 30th International Electric Propulsion Conference, Florence, Italy, 17-20 September 2007, Paper No. IEPC-2007-188.
[57] Hoskins, A., Personal Communication, December 2008.
[58] Mirels, H., Rosenbaum, B. M., "Analysis of One-Dimensional Ion Rocket," NASA TN D-266, 1960.
[59] Kaufman, H. R., "One-Dimensional Analysis of Ion Rockets," NASA TN D-261, 1960.
[60] Byers, D. C., "Angular Distribution of Kaufman Ion Thruster Beams," NASA TN D-5844, 1970.
[61] Nieberding, W. C., Lesco, D. J., Berkopec, F. D., "Comparative In-Flight Thrust Measurements of the SERT II Ion Thruster," AIAA 8th Electric Propulsion Conference and Exhibit, August 31–September 2, 1970, Stanford, CA, Paper No. AIAA 75-405.
[62] Kerslake, W. R., Goldman, R. G., Nieberding, W. C., "SERT II: Mission, Thruster Performance, and In-Flight Thrust Measurements," *Journal of Spacecraft*, Vol. 8, No. 3, March 1971, pp. 213-224.
[63] Banks, B., Rawlin, V., Weigand, A., Walker, J., "Direct Thrust Measurement of a 30-cm Ion Thruster," NASA TM X-71646.
[64] Brophy, J. R., "NASA's Deep Space 1 Ion Engine (plenary)," *Review of Scientific Instruments*, Vol. 73, No. 2, Feb. 2002, pp. 1071-1078.
[65] Brown, D. L., "Investigation of Low Discharge Voltage Hall Thruster Characteristics and Evaluation of Loss Mechanisms," Ph.D. Dissertation, University of Michigan, Ann Arbor, Michigan, 2009.
[66] Azziz, Y., "Experimental and Theoretical Characterization of a Hall Thruster Plume," Ph.D. Dissertation, Massachusetts Institute of Technology, Cambridge, Massachusetts, 2007.
[67] Shastry, R., Hofer, R. R., Reid, B. M., Gallimore, A. D., "Method for Analyzing ExB Probe Spectra from Hall Thruster Plumes," 44rd AIAA/ASME/SAE/ASEE Joint Propulsion Conference and Exhibit, 21-23 July, 2008, Hartford, CT, Paper No. AIAA 2008-4647.
[68] Reid, B. M., Shastry, R., Gallimore, A. D., Hofer, R. R., "Angularly-Resolved ExB Probe Spectra in the Plume of a 6 kW Hall Thruster," 44rd AIAA/ASME/SAE/ASEE Joint Propulsion Conference and Exhibit, 21-23 July, 2008, Hartford, CT, Paper No. AIAA 2008-5287.
[69] Kim, S. W., "Experimental Investigations of Plasma Parameters and Species-Dependent Ion Energy Distribution in the Plasma Exhuast of a Hall Thruster," Ph.D. Dissertation, University of Michigan, Ann Arbor, Michigan, 1999.
[70] Beal, B. E.. "Clustering of Hall Effect Thrusters for High Power Electric Propulsion Applications," Ph.D. Dissertation, University of Michigan, Ann Arbor, Michigan, 2004.